Pakistan J. Zool., pp 1-12, 2023. **DOI**: https://dx.doi.org/10.17582/journal.pjz/20220923120947

Alpha-2-Macroglobulin and Alpha-2-HS Glycoprotein are Potential Markers of Renal Cell Carcinoma: An Insight from Proteome Profile of Cancer Tissues

Safa Akhtar[1,3], Shahzadi Noreen[2], Anna E. Lokshin[3] and Muhammad Waheed Akhtar[1]*

[1]*School of Biological Sciences, University of the Punjab, Quaid-I-Azam Campus, Lahore 54590, Pakistan*
[2]*Department of Science, International Institute of Science, Arts and Technology, Gujranwala 52250, Pakistan*
[3]*University of Pittsburgh Cancer Institute, Hillman Cancer Center, 5117 Centre Avenue 1.18, Pittsburgh, PA, 15213*

Article Information
Received 03 February 2023
Revised 15 February 2023
Accepted 21 February 2023
Available online 28 August 2023
(early access)

Authors' Contribution
MWA supervised the study. AEL provided all the facilities in foreign lab and helped in conducting the multiplex assays. SA performed the experimental work and prepared the manuscript. SN provided assistance in analysis of the data

Key words
Renal cell carcinoma, Protein biomarkers, LC-MS/MS, Multiplex bead-based immunoassay, Immunohistochemistry

ABSTRACT

Renal cell carcinoma (RCC) is characterized as the most common neoplasm of the human kidney among the top fifteen most diagnosed tumors, encompassing multiple subhistologies with definite genomic, clinicopathological, genomic and proteomic features. Proteomics technologies enable the detection and quantitation of protein profiles associated with RCC to delineate the dysregulated expression of various proteins involved in multiple cellular processes. In this study, which is novel for local population, we employed liquid chromatography-tandem mass spectrometry (LC-MS/MS) analysis to characterize proteome profiles of the tissue and the serum samples obtained from RCC patients. Five paired (RCC and adjacent normal) and 2 pooled sets of samples were utilized. Out of the 3,167 identified proteins from MS spectra 78 of interest (p value ≤ 0.05; 0.9 % protein decoy FDR; 0.07 % peptide decoy FDR; fold change ≥ 1) were selected through scaffold analysis with up regulated expression of 42 proteins in tumor along with 36 downregulated proteins. From the panel of 13 proteins i.e. ACTG2, A2M, FETUA, CAP1, OSTF1, RL32, PDLI1, GBB1, MAP1B, RL30, PIMT, C163A, SC22B and SMD3 that were not previously reported in RCC, two proteins; alpha -2-macroglobulin (A2M) and alpha-2-HS glycoprotein (FetuA) were subjected to validation through multiplexed analysis by Luminex and immunohistochemistry. We found upregulated expression of A2M (2.6 folds) and FetuA (1.6 folds) along with decreased serum excretion (P=0.0061) (P=0.0002) in RCC patients, respectively. The expression was validated through histochemical studies of the tissue samples. Further studies on larger sample size and rich validity cohort shall elucidate the role of A2M and FetuA to serve as novel therapeutic interventions for RCC.

INTRODUCTION

Renal cell carcinoma (RCC) encompasses a diversified group of tumors consisting of different histological variants with a definite genetics, clinical course and response of patients to different treatment strategies. The tumor originates from renal tubular epithelial cells and is delineated among ten most frequently diagnosed cancers worldwide (Loomans-Kropp and Umar, 2019). The majority of cancer associated deaths have been attributed to the clear cell renal cell carcinoma that represent 75% of all cases (Clark *et al*., 2019). Major emendations in the classification of RCC is the outcome of scientific advances in histopathological and molecular characterization of the disease over the past twenty years. It is a common nephrological tumor that accounts for 3% of all human malignancies with significantly enhanced prevalence and mortality as compared to the other urological tumors (El-Shorbagy and Alshenawy, 2017). Proteomic technologies

* Corresponding author: mwa.sbs@pu.edu.pk
0030-9923/2023/0001-0001 $ 9.00/0

Abbreviations
A2M, alpha-2-macroglobulin; FetuA, alpha-HS-glycoprotein; IHC, immunohistochemistry; LC-MS/MS, liquid chromatography-tandem mass spectrometry; PANTHER, protein analysis through evolutionary relationships; STRING, search tool for the retrieval of interacting genes; RCC, renal cell carcinoma.

have been utilized in a myriad of studies to traverse the protein profiles of biological fluids and tissues in an attempt to identify and characterize the differentially expressed proteins in RCC. The dysregulated protein expression that results from aberrant gene expressions in RCC is characterized through analysis of tumor tissues by employing different proteomic approaches (Clark and Zhang, 2020). Comparative proteomic profiling facilitates the identification of differentially expressed proteins through the study of tumor and normal adjacent tissue with the aim of elucidating potential protein biomarkers for the disease (Macklin *et al*., 2020). In context of clinical proteomics, mass spectrometry based platforms have been extensively used for testing and validation of a large number of candidate biomarkers for RCC. Increased proteome coverage along with reliable quantitation is made possible through recent expansions in LC–MS technology thus, providing the most precise contemplation of the physiological state of tumor through the tissue analysis. These studies have been implicated for routine proteomics analyses of patient tumor tissues in an attempt to discover various biomarkers, different biological pathways integrating accessible genomics or transcriptomics profiles (Al-Wajeeh *et al*., 2020). The current study was aimed to identify the expression patterns of different disease related proteins in tumor and normal tissues of RCC employing various proteomic based approaches. Pathway analyses was done that give insight into associations of the proteins with tumorigenesis, proliferation and with other proteins. We performed multiplex analysis to validate the differential expression of proteins in an independent cohort along with IHC studies to understand the spatial information regarding the proteins. Our work encompasses approaches and future directions that provide insight to study various altered protein expressions that could be viewed as a valuable new biomarkers for RCC.

MATERIALS AND METHODS

Sample collection and processing

From the local hospitals of Lahore, Pakistan, blood samples of the pre-operative RCC patients along with age-matched healthy study participants were collected into EDTA containing vacutainers after approval of the project by university ethical review committee [Ref. No. 873/12]. Serum was separated immediately by centrifugation at 12,000 rpm for 10 min at 4 °C and stored in aliquots at -80 ºC until further processing. The complete clinical history of the patients with the tumor stage range pT2 to pT4 was recorded. Patients with any prolonged disease history including HBV, HCV, HIV and/or chemo-/radiotherapy were not taken in the study. Tissue samples of RCC patients were stored in liquid nitrogen immediately after surgical resection. Pathologically the tissues comprising of at least 60-80 % tumor cells were considered tumorous whereas adjacent tissues, taken 10 cm away from the tumor site, free of any cancer cell were labelled as healthy controls. Furthermore, 3 formalin fixed paraffin embedded tissues were selected for immunohistochemistry for the validation of selected proteins.

Tissue homogenization

After thorough washing of RCC and adjacent normal tissues (0.4–1.0 g) with ice cold phosphate-buffered saline (PBS), homogenization was performed in a bead based (Precellys 24) homogenizer in a chilled lysis buffer [6 mol/L urea, 2 mol/L thiourea, 65 mmol/L dithiothreitol (DTT), iodoacetamide (IAA), cholamidopropyldimethylammonio-propanesulfate (CHAPS) (4%), servalyte (2%) (Amersham Biosciences)] (Huang *et al*., 2014). The homogenates were then vortexed for 30 min and cell debris were removed by centrifugation at 14,000 rpm for 1 h at 4 °C. Supernatants (tissue lysates) were stored in aliquots at -80 °C until use.

Protein estimation

Protein quantification was done by the Bradford method in a 96 well plate and Bio-Tek uQuant with KC junior software was used for analysis. Furthermore, 12% SDS-PAGE was done according to the previously described protocol (Bradford, 1976) to get a preview of the differential proteome profile of the study subjects.

LC-MS/MS analysis

For LC-MS/MS analysis, tissue homogenates were dissolved in 100 mM ammonium bicarbonate buffer containing 2 M urea. After vigorous vortexing, the homogenates were reduced by adding 5 mM DTT for 30 min at room temperature followed by alkylation with 15 mM IAA in dark. Urea concentration was reduced by further dilution of the homogenates with ammonium bicarbonate buffer and proteins in them were digested by overnight incubation with 20 ng/µL trypsin solution in 50 mM ammonium bicarbonate. Next day, the digestion was stopped by 10 % formic acid. For proteomic analysis 12 digests were prepared comprising of 10 samples [paired groups of RCC tumor and adjacent normal tissue digests) and 2 sets of pooled samples combined normal lysates (group A)] and combined tumor extracts (group B). SDS-PAGE was run for both tryptic and non-tryptic digests to ensure the complete digestion.

Sample analysis was done through Fusion mass spectrometer (Thermo Scientific) equipped with a nanospray Flex Ion Source (Thermo Scientific) for ionization. Peptide separation was done through Reversed-phase chromatography (Acclaim PepMap100

C18 column, Thermo Scientific) along with collision-induced dissociation (CID) for fragmentation. Mass data were acquired using Proteome Discoverer 2.1 (Thermo) with incorporated Sequest algorithm (Thermo Fisher). Uniprot_Hum_Compl_20170714 database was utilized for the search of human protein sequences. For FDR determination reverse decoy protein database was run simultaneously. The search parameters selected for LC-MS/MS analysis were; ion tolerance of 10 PPM, fragment mass tolerance of 0.6 Da, fixed modification in Sequest and X! (Carbamido methylation of cys), and variable modification (Deamidation of Asn and Gln, oxidation of Met, and acetylation of the N-terminus). Data was processed using Scaffold (proteome software sf3) and a subset database was searched using X! Tandem. Spectral counts were used to determine the abundant proteins.

In silico functional analysis of proteins

Protein-protein interactions were predicted through the retrieval of interacting genes/proteins via string (http://www.string-db.org/) (Szklarczyk and Jensen, 2015). Further analysis of proteome data in terms of gene ontology was done through the comprehensive database (http.//www.pantherdb.org/) for classification (Mi *et al*., 2013). Analyses were performed for all the significant proteins identified through LC-MS/MS.

Immunological assays

Luminex

The target proteins A2M and FetuAwere analyzed through multiplexed approach using Bio-Plex Suspension Array System (Bio-Rad) based on the Luminex platform. Assay kits were purchased from EMD Millipore (Billerica, MA). All assays were performed in duplicates according to manufacturers protocols as described earlier. The data was analyzed by five parametric curve fitting method (Bio-Rad) (Shaw *et al*., 2022).

Immunohistochemical analysis

Formalin-fixed, paraffin-embedded 4 mm thick sections mounted on positively charged slides were taken for immunohistochemistry. Tissue sections were deparaffinized and rehydrated by PT Link apparatus (Dako, Glostrup, Denmark). Incubation was done for 20 min at 97°C with low pH, by using antigen retrieval solution (Dako). A robotic platform (Autostainer, Dako) was used to perform Immunohistochemistry (IHC). Antibodies for A2M (Ab 109422), FetuA (Ab 187051) were obtained from Abcam, USA. 1:100 diluation of antibody was used. Antigen–antibody complex detection was done by the use of Envision TM Dual Link (Dako) followed by incubation with 3, 3'-diaminobenzidine tetrahydrochloride (DAB+) chromogen (Dako). For assessment all the slides were counterstained with hematoxylin followed by dehydration and slide mounting. Slides were observed for the positive and negative reaction of antibody with the target tissues. The extent of immunoreactivity was analyzed by scoring the extent of the staining intensity as follows: 0 means no staining, 1 indicates weak, 2 representing the moderate while 3 illustrates strong staining. The quartile score assigned to the percentage of stained tumor cells elucidated as no staining = 0, 1-25%=1, 26-50%= 2, 51-75% =3 and 76-100% =4. Score index was calculated after multiplying two scores for each case (Range 1-12).

Statistical analysis

Statistical analysis was done through SPSS ver. 15.0 (IBM Corporation, Armonk, NY) and GraphPad Prism 6.01 for calculation of individual protein concentration means, standard deviation (SD), and standard error (SE) values. The concentration of each protein for tumorous and normal controls were assessed through descriptive statistical analysis and dot plots. Individual comparisons were done by Mann-Whitney test. For analysis of the classification potential of biomarkers ROC analysis was done.

RESULTS

Protein profile of RCC

Table I shows clinicopathological features of RCC patents. Protein concentrations of the tryptic digested tissue lysates and their corresponding non digested samples was estimated by Bradford plate Assay and SDS-PAGE (Fig. 1). The average protein concentrations varied from 0µg/ml (Blank) to 10 µg/ml (lysates) (Fig. 1A). The plot between concentration and absorbance values was obtained by KC junior software (Fig. 1B). The lanes clear of any protein band on SDS-PAGE indicated the complete tryptic digestion for LC-MS/MS analysis (Fig. 1C).

Table II shows the variety of proteins identified in RCC tissue lysate by LC-MS/MS analysis. Identification of proteins was completed on account of spectral counts. A total of 3,167 total proteins were identified from 224,607 MS2 spectra. Following parameters were set for minimum protein identification probability i.e. ≤ 1.0% FDR with 2 unique peptides at ≤ 1.0% FDR minimum peptide identification probability (0.9% protein decoy FDR, 0.07% peptide decoy FDR). Significance was viewed as +/- issue rather than a more/less issue. Proteins of interest were selected according to p value < 0.05 as 1st cut, while "difference in abundance" was the 2nd cut for the selection of potential proteins for further evaluation studies. Out of 3167 identified proteins, 78 proteins showed

Table I. Clinicopathological features of renal cell carcinoma patients.

Sample No.	Gender	Age (Years)	Tumor size (cm)	Lymph node metastasis	Liver metastasis	*TNM staging
1	Male	65	12	P	P	T4N2M1
2	Male	55	7.5	P	P	T4N2M1
3	Female	51	8	P	A	T4N2M0
4	Male	38	10	P	A	T4N1M0
5	Male	48	13	P	A	T3N1M0
6	Male	53	17	P	P	T4N2M1
7	Female	47	6.5	P	A	T3N1M0
8	Female	55	8	A	A	T3N0M0
9	Female	63	9	A	A	T3N0M0
10	Female	75	13.5	A	A	T2N0M0
11	Male	41	10	P	A	T3N1M0
12	Male	70	11	A	A	T2N0M0
13	Male	67	5.5	P	A	T2N1M0
14	Female	33	8	A	A	T3N0M0
15	Male	61	10	P	A	T4N2M0
16	Male	42	8	P	A	T2N1M0
17	Female	58	9.5	P	A	T3N1M0
18	Female	54	18	P	P	T4N2M1
19	Female	63	27	P	P	T4N2M1
20	Female	51	11.5	P	A	T3N1M0

*TNM- Tumor, Node, Metastasis, *P Present, A Absent.
Tumor stages were evaluated by pathologists according to AJCC/UICC recommendation.

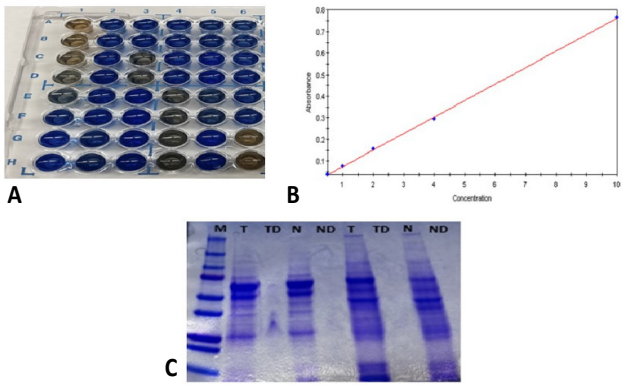

Fig. 1. (A) Bradford plate assay. (B) Estimation of protein concentration of tryptic digested and non digested lysates by microplate quantification assay. (C) SDS-PAGE analysis of tryptic digests and non digested tissue lysates M symbolizes the ladder T and TD represent tumor and tumor digest, respectively whereas N and ND symbolize Normal and normal digest.

significant p value less than 0.05 and fold value greater than 1 (Table II). After analysis through scaffold forty-two proteins were found to be overexpressed in tumor samples while thirty-six proteins showed lower expression in malignant samples and were up regulated in normal samples. The identification of proteins was done on the basis of exclusive spectrum counts for each sample. The proteins such as adenylyl cyclase-associated protein 1(CAP1), alpha-2-HS-glycoprotein (FETUA), osteoclast-stimulating factor 1(OSTF1), 60S ribosomal protein L32 (RL32), PDZ and LIM domain protein 1(PDLI1), guanine nucleotide-binding protein G(I)/G(S)/G(T) subunit beta-1(GBB1), microtubule-associated protein 1B(MAP1B), 60S ribosomal protein L30 (RL30), protein-L-isoaspartate(D-aspartate) O-methyltransferase (PIMT), scavenger receptor cysteine-rich type 1 protein M130 (C163A), plastin-2 (PLSL), vesicle-trafficking protein SEC22b (SC22B), small nuclear ribo nucleoprotein Sm D3 (SMD3) and alpha-2-macroglobulin (A2M) were not found to be associated with RCC in any previous studies suggesting their potential as differential protein markers and need to be further analyzed. The quantitative profile, protein sequence coverage and spectrum were retrieved from Scaffold (Fig. 2A, B). The results for Scaffold and Orbitrap files can be accessed using the information (http:// 141.217.61.1/Lokshin username = lokshin, Password = lokshin123).

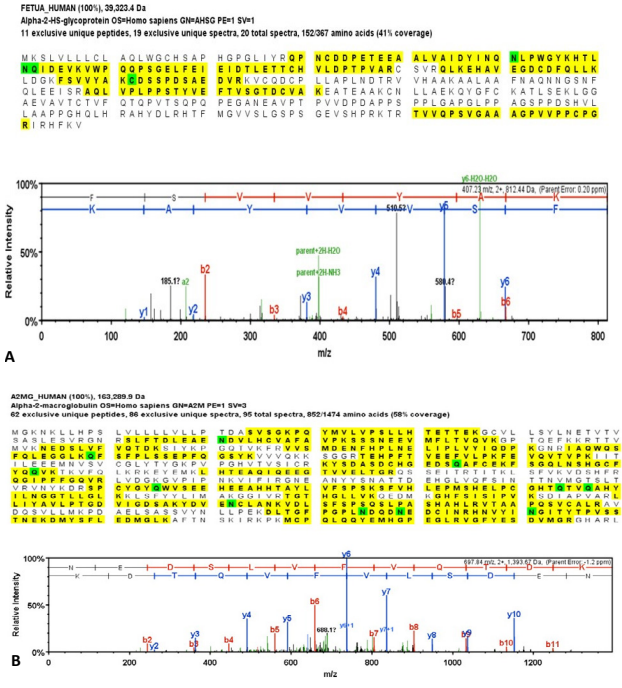

Fig. 2. Mass spectrometric analysis of proteins with 99% Minimum 2 Min # Peptides 0.9% Decoy FDR; Spectra at 85.0 % Minimum 0.07% Decoy FDR for (A)- Alpha-2 HS glycoprotein (FETUA), (B)- Alpha-2 macroglobulin.

Table II. Protein identification in (RCC) tissue lysates by LC-MS/MS analysis.

S. No	Identified proteins	accession number	Molecular weight KDa	T-test (p value): *(p<0.05)	Fold change by category	Quantitative profile
1.	Vimentin	VIME_HUMAN	54 kDa	0.0012	1.8	Normal low, Tumor high
2.	Neuroblast differentiation-associated protein AHNAK	AHNK_HUMAN	629 kDa	0.04	1.7	Normal high, Tumor low
3.	Pyruvate kinase PKM	KPYM_HUMAN	58 kDa	0.0027	2.4	Normal low, Tumor high
4.	Alpha-2-macroglobulin	A2MG_HUMAN	163 kDa	0.0091	2.4	Normal low, Tumor high
5.	L-lactate dehydrogenase A chain	LDHA_HUMAN	37 kDa	0.035	1.8	Normal low, Tumor high
6.	Ceruloplasmin	CERU_HUMAN	122 kDa	0.031	2.3	Normal low, Tumor high
7.	Fructose-bisphosphate aldolase A	ALDOA_HUMAN	39 kDa	0.00063	1.9	Normal low, Tumor high
8.	Glucose-6-phosphate isomerase	G6PI_HUMAN	63 kDa	0.057	1.6	Normal low, Tumor high
9.	Ras GTPase-activating-like protein IQGAP1	IQGA1_HUMAN	189 kDa	0.0076	1.5	Normal low, Tumor high
10.	78 kDa glucose-regulated protein	GRP78_HUMAN	72 kDa	0.024	1.5	Normal low, Tumor high
11.	Fibronectin	FINC_HUMAN	263 kDa	0.0063	1.9	Normal low, Tumor high
12.	Laminin subunit beta-2	LAMB2_HUMAN	196 kDa	0.034	2.7	Normal high, Tumor low
13.	Histone H2B type 1-H	H2B1H_HUMAN	14 kDa	0.0017	1.5	Normal low, Tumor high
14.	Neutral alpha-glucosidase AB	GANAB_HUMAN	107 kDa	0.051	1.5	Normal high, Tumor low
15.	Annexin A1	ANXA1_HUMAN	39 kDa	0.025	1.7	Normal high, Tumor low
16.	Adenylyl cyclase-associated protein 1	CAP1_HUMAN	52 kDa	0.027	1.5	Normal high, Tumor low
17.	Alpha-2-HS-glycoprotein	FETUA_HUMAN	39 kDa	0.0024	1.6	Normal low, Tumor high
18.	Prolow-density lipoprotein receptor-related protein 1	LRP1_HUMAN	505 kDa	0.028	4.3	Normal high, Tumor low
19.	Protein-glutamine gamma-glutamyltransferase 2	TGM2_HUMAN	77 kDa	0.025	8	Normal high, Tumor low
20.	ATP-dependent 6-phosphofructokinase, platelet type	PFKAP_HUMAN	86 kDa	0.00039	10	Normal low, Tumor high
21.	Glycogen phosphorylase, brain form	PYGB_HUMAN	97 kDa	0.014	2.6	Normal high, Tumor low
22.	Inter-alpha-trypsin inhibitor heavy chain H2	ITIH2_HUMAN	106 kDa	0.0097	2.6	Normal low, Tumor high
23.	Calnexin	CALX_HUMAN	68 kDa	0.042	1.9	Normal low, Tumor high
24.	Stress-induced-phosphoprotein 1	STIP1_HUMAN	63 kDa	0.047	1.5	Normal high, Tumor low
25.	Galectin-1	LEG1_HUMAN	15 kDa	0.0083	2.8	Normal low, Tumor high
26.	Inter-alpha-trypsin inhibitor heavy chain H1	ITIH1_HUMAN	101 kDa	0.027	2	Normal high, Tumor low
27.	Myristoylated alanine-rich C-kinase substrate	MARCS_HUMAN	32 kDa	0.044	1.9	Normal high, Tumor low
28.	Nidogen-2	NID2_HUMAN	151 kDa	0.032	7.8	Normal high, Tumor low
29.	Thymidine phosphorylase	TYPH_HUMAN	50 kDa	0.047	2.9	Normal high, Tumor low
30.	Inter-alpha-trypsin inhibitor heavy chain H4	ITIH4_HUMAN	103 kDa	0.042	2.8	Normal high, Tumor low
31.	Septin-2	SEPT2_HUMAN	41 kDa	0.023	1.5	Normal high, Tumor low
32.	Laminin subunit alpha-4	LAMA4_HUMAN	203 kDa	0.0059	8.5	Normal low, Tumor high

Table continued on next page.....

S. No	Identified proteins	accession number	Molecular weight KDa	T-test (p value): *(p<0.05)	Fold change by category	Quantitative profile
33.	40S ribosomal protein SA	RSSA_HUMAN	33 kDa	0.003	1.7	Normal high, Tumor low
34.	Calpain small subunit 1	CPNS1_HUMAN	28 kDa	0.036	1.5	Normal high, Tumor low
35.	Fructose-bisphosphate aldolase C	ALDOC_HUMAN	39 kDa	0.00047	2.5	Normal low, Tumor high
36.	DNA damage-binding protein 1	DDB1_HUMAN	127 kDa	0.0089	1.8	Normal low, Tumor high
37.	Aldose reductase	ALDR_HUMAN	36 kDa	0.0057	2.1	Normal low, Tumor high
38.	Septin-9	SEPT9_HUMAN	65 kDa	0.022	2.1	Normal high, Tumor low
39.	Multifunctional protein ADE2	PUR6_HUMAN	47 kDa	0.047	2.1	Normal high, Tumor low
40.	Proliferation-associated protein 2G4	PA2G4_HUMAN	44 kDa	0.0037	1.8	Normal low, Tumor high
41.	Microtubule-associated protein 4	MAP4_HUMAN	121 kDa	0.048	2.5	Normal low, Tumor high
42.	Gamma-enolase	ENOG_HUMAN	47 kDa	0.0097	2.9	Normal low, Tumor high
43.	Calumenin	CALU_HUMAN	37 kDa	0.012	3.5	Normal low, Tumor high
44.	Glycogen phosphorylase, liver form	PYGL_HUMAN	97 kDa	<0.00010	28	Normal low, Tumor high
45.	Coronin-1C	COR1C_HUMAN	53 kDa	0.013	2.1	Normal low, Tumor high
46.	40S ribosomal protein S3	RS3_HUMAN	27 kDa	0.024	1.5	Normal high, Tumor low
47.	N-acetyl-D-glucosamine kinase	NAGK_HUMAN	37 kDa	0.025	2.4	Normal high, Tumor low
48.	40S ribosomal protein S4, X isoform	RS4X_HUMAN	30 kDa	0.032	1.5	Normal high, Tumor low
49.	Serpin H1	SERPH_HUMAN	46 kDa	0.00053	2.1	Normal low, Tumor high
50.	Microtubule-associated protein 1B	MAP1B_HUMAN	271 kDa	0.0004	22	Normal low, Tumor high
51.	Caveolae-associated protein 1	CAVN1_HUMAN	43 kDa	0.0021	2.9	Normal low, Tumor high
52.	Fatty acid-binding protein, epidermal	FABP5_HUMAN	15 kDa	0.0013	5.8	Normal low, Tumor high
53.	HLA class I histocompatibility antigen, A-68 alpha chain	1A68_HUMAN	41 kDa	0.042	3.5	Normal high, Tumor low
54.	40S ribosomal protein S3a	RS3A_HUMAN	30 kDa	0.02	1.9	Normal high, Tumor low
55.	Glycogen debranching enzyme	GDE_HUMAN	175 kDa	0.055	2.8	Normal high, Tumor low
56.	Proteasome subunit alpha type-7	PSA7_HUMAN	28 kDa	0.013	2	Normal high, Tumor low
57.	Tripeptidyl-peptidase 1	TPP1_HUMAN	61 kDa	0.054	1.9	Normal high, Tumor low
58.	PDZ and LIM domain protein 1	PDLI1_HUMAN	36 kDa	0.027	2.7	Normal high, Tumor low
59.	14-3-3 protein eta	1433F_HUMAN	28 kDa	0.0016	1.9	Normal low, Tumor high
60.	Guanine nucleotide-binding protein G(I)/G(S)/G(T) subunit beta-1	GBB1_HUMAN	37 kDa	0.019	1.5	Normal low, Tumor high
61.	NADH-cytochrome b5 reductase 3	NB5R3_HUMAN	34 kDa	0.038	3.9	Normal high, Tumor low
62.	Proteasome subunit beta type-4	PSB4_HUMAN	29 kDa	0.028	1.9	Normal high, Tumor low
63.	EGF-containing fibulin-like extracellular matrix protein 1	FBLN3_HUMAN	55 kDa	0.085	1.9	Normal high, Tumor low
64.	RNA-binding motif protein, X chromosome	RBMX_HUMAN	42 kDa	0.064	2.1	Normal high, Tumor low
65.	EH domain-containing protein 2	EHD2_HUMAN	61 kDa	0.045	7.3	Normal high, Tumor low
66.	Thymosin beta-4	TYB4_HUMAN	5 kDa	0.019	2.8	Normal high, Tumor low
67.	Periostin	POSTN_HUMAN	93 kDa	0.027	5.2	Normal high, Tumor low
68.	Aspartyl aminopeptidase	DNPEP_HUMAN	52 kDa	0.042	2	Normal high, Tumor low

Table continued on next page.....

S. No	Identified proteins	accession number	Molecular weight KDa	T-test (p value): *(p<0.05)	Fold change by category	Quantitative profile
69.	Fascin	FSCN1_HUMAN	55 kDa	0.0057	3.3	Normal low, Tumor high
70.	40S ribosomal protein SA	RSSA_HUMAN	33 kDa	0.003	1.7	Normal low, Tumor high
71.	Plastin-2	PLSL_HUMAN	70 kDa	0.0058	3	Normal low, Tumor high
72.	Osteoclast-stimulating factor 1	OSTF1_HUMAN	24 kDa	0.0043	3.5	Normal low, Tumor high
73.	Protein-L-isoaspartate (D-aspartate) O-methyltransferase	PIMT_HUMAN	25 kDa	0.002	1.9	Normal low, Tumor high
74.	Scavenger receptor cysteine-rich type 1 protein M130	C163A_HUMAN	125 kDa	0.0029	6.3	Normal low, Tumor high
75.	Vesicle-trafficking protein SEC22b	SC22B_HUMAN	25 kDa	0.0046	1.7	Normal low, Tumor high
76.	Small nuclear ribonucleoprotein Sm D3	SMD3_HUMAN	14 kDa	0.0024	5.5	Normal low, Tumor high
77.	60S ribosomal protein L32	RL32_HUMAN	16 kDa	0.0081	2.4	Normal low, Tumor high
78.	60S ribosomal protein L30	RL30_HUMAN	13 kDa	0.0001	3.8	Normal low, Tumor high

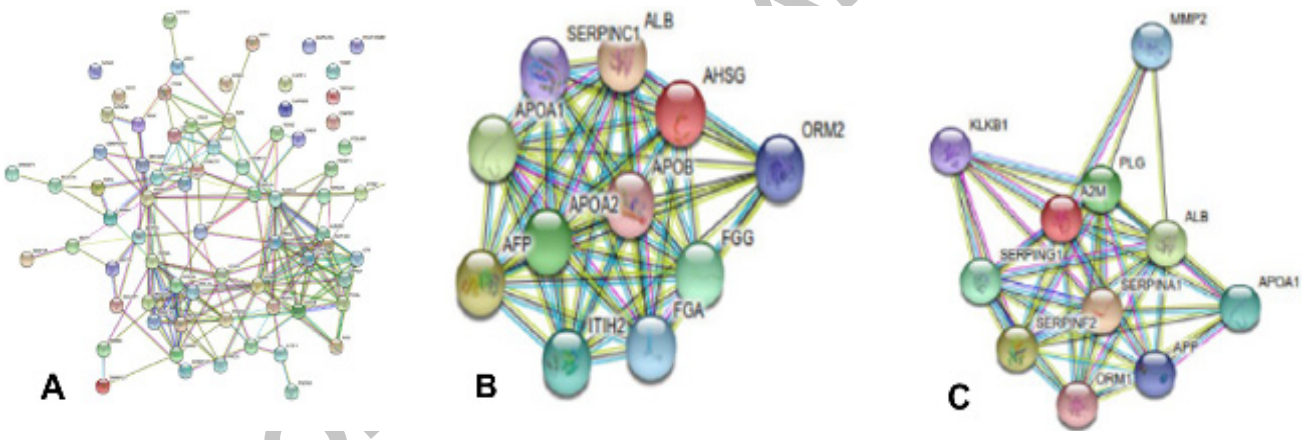

Fig. 3. (A) STRING analysis of differentially expressed proteins that were identified through LC-MS/MS in RCC. UniProt ID of 78 proteins were added in the category of multiple protein. The viewed evidence was shown in different coloured lines to indicate type of evidence in order to support each interaction. STRING analysis showed more interaction among set of protein than expected indicating that proteins were partially connected biologically. Protein interaction maps of B)- AHSG (FetuA).and C)- A2M.

Network and functional analysis through computational tools

Network analysis (confidence scores > 0.7) give information about the key interacting protein partners and pathways in which present data set proteins are involved in the cell characterizing diversified functional landscape of all the potential significant proteins identified in RCC (Fig. 3).

Functional analysis by Panther categorized differentially represented proteins according to various molecular functions, including catalytic activity (32.4%), binding (48.1%), molecular function regulator (10/8%), receptor activity (4.3%), structural molecule activity (9.5%) and molecular transducer activity (1.4%) (Fig. 4A). The proteins showed clear associations with ten main divisions of biological processes in terms of biological adhesion (4.3%), biological regulation (12.2%), cellular component organization or biogenesis (2.7%), cellular processes (37.6%), developmental process (2.7%), metabolic process (22.6%), localization (10.8%), immune system process (2.7%), multicellular organismal process (9.5%), response to stimulus (4.1%) (Fig. 4B).

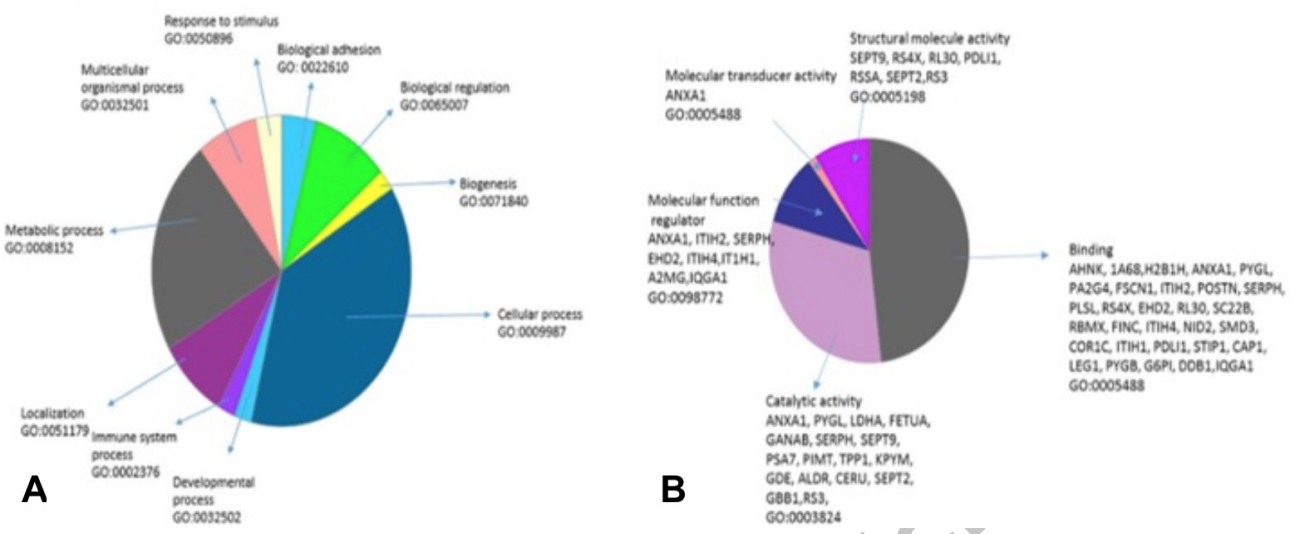

Fig. 4. Protein categorization through panther analysis: A, biological processes; B, molecular functions.

Multiplexed analysis

Bead-based multiplex analysis was used to evaluate the concentrations of A2M and FETUA in the sera of patients diagnosed with RCC (n=20) along with healthy individuals (n=46) (Fig. 5). Dot plots were generated by Graphpad Prism for the comparison of serum levels of proteins. In contrast to the LC-MS/MS results low concentrations of A2M (P= 0.0061) and FetuA (P= 0.0002) were reported in RCC patients as compared to the normal (Fig. 4).

Multiplexed analysis

Bead-based multiplex analysis was used to evaluate the concentrations of A2M and FETUA in the serum samples of patients diagnosed with RCC (n=20) along with healthy individuals (n=46). Dot plots were generated by Graphpad Prism to compare the serum levels of proteins in RCC and normal controls. In contrast to the LC-MS/MS results low levels of A2M (P=0.0061) and FetuA (P=0.0002) were obtained in RCC patients's srea as compared to the normal (Fig 5A, B).

Immunological verification of A2M and FetuA in RCC tissues

Since differential regulation of A2M and FetuA had not previously been found associated with RCC, their levels were further assessed in the tissues of RCC and normal tumor adjacent tissues by IHC. Histochemical anaysis showed the greater abundance of A2M (P-value < 0.05 and fold change of 2.4) and FetuA (P= 0.002 and 1.6 fold change) in RCC tissues as compared to the normal tissues (Fig. 5C, Table III) confirming LC-MS/MS results.

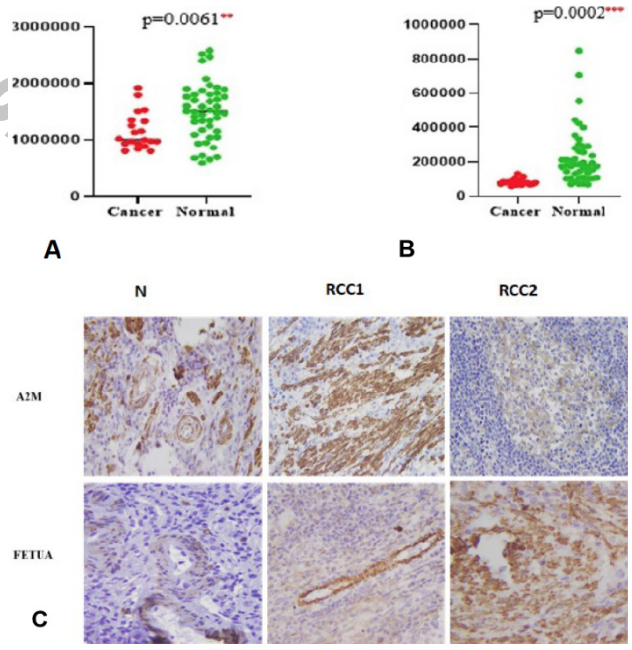

Fig. 5. Dot plots of Luminex for A2M (A) and FetuA (B). C, IHC analysis of upregulated proteins A2M and FetuA in RCC and normal tissue.

DISCUSSION

Renal cell carcinoma (RCC) is the most invasive form of adult kidney malignancy that results in more than 100,000 annual deaths globally due to fatal prognosis (Hussain *et al.*, 2019). The high mortality rate is due to lack of symptoms and distinctive screening factors for

Table III. Immunohistochemical score calculation for A2M and FETUA in RCC and adjacent normal tissue.

Sample no	Protein	Normal			Tumor		
		IHC intensity	Quartile cells staining	IHC score*	IHC Intensity	Quartile cells staining	IHC score*
1	A2M	2	4	8	3	4	12
2		2	4	8	3	3	9
1	FetuA	1	2	2	2	2	4
2		1	2	2	2	3	6

RCC at initial stages. Furthermore, distant invasion, and metastasis are the key factors involved in high death rates in developing countries (Siegel *et al*., 2021). Therefore the identification of predictive biomarkers for early diagnosis is the need of time to study the underlying mechanism of the disease progression and to establish the improved treatment options for tumor patients (Rini *et al*., 2021).

Use of proteomic strategies based on tissue analysis have been extensively used to the study various cancers including prostate (Kwon *et al*., 2020), breast (Mardamshina and Geiger, 2017), melanoma (Surman *et al*., 2020), lungs (Gasparri *et al*., 2020), ovarian (Dutta *et al*., 2021) and oropharyngeal carcinoma (Drápela *et al*., 2021). The comparative analysis of cancerous tissue samples with adjacent normal tissues done through clinical proteomic provide insight to access the varying stages of cancer for the prognosis and development of potential biomarkers (Baran and Brzeziańska-Lasota, 2021).

In the present study we aimed to characterize the molecular markers for RCC diagnosis with ongoing current technologies in the area of Omics. RCC samples were analyzed with LC-MS/MS analysis coupled with immune validational analysis by multiplexing and IHC along with different computational analysis for functional studies. Among a total of 3167 proteins identified, 78 significant proteins were selected with P value ≤ 0.05 by scaffold analysis. Among them, 42 proteins were found overexpressed while 36 proteins were found to be down regulated in RCC samples (Table II). These differentially expressed proteins were found to be directly linked to the alterations in different metabolic pathways crucial for disease progression (Fig. 4).

Two proteins identified in present work viz. FetuA and A2M whose differential abundance had not been previously reported in RCC were selected for validation by immunohistochemical and multiplex analysis. A2M is synthesized in liver act as inhibitor of different metalloproteases, thrombin, threonine, serine and other inflammatory cytokines. The A2M controls tumor cell migration and invasion (Mekkawy *et al*., 2014) and its blood levels are negatively correlated with age (Thieme *et al*., 2015). The protein was reported to induce the transcriptional activation of genes responsible for oncogenesis, atherosclerosis and hypertrophy of cells (Yoshino *et al*., 2019). Previously complications in nephrotic system such as increased viscosity of plasma along with decreased zinc availability had been attributed mainly to enhanced levels of A2M (McGinley *et al*., 1983).

In the present work, increased expression of A2M (2.4 fold) in tumor tissues was observed compared to the adjacent normal tissues. Interestingly, significantly reduced levels were found in sera of RCC patients (P=0.0061) when multiplexed analysis was performed (Fig. 5). Previously, an increased expression of A2M synthesis was reported in nephrotic rats but in humans the mechanism for A2M expression in plasma requires further elucidation (Stevenson *et al*., 1998). In other diseases such as diabetes mellitus increased serum level of A2M act as a mediator for albuminuria progressing towards cardiovascular diseases (Garcia-Fernandez *et al*., 2020). Peers reported decreased A2M plasma levels in humans with age along with inhibition of many cancer associated attributes of tumor cells mainly due to inhibition of WNT/ß-catenin pathway. The study suggested that reduction of A2M may trigger the tumor development in aged people (Lauer *et al*., 2001). Moreover, due to its high binding affinity, A2M was the controlling agent in the removal of TGF-ß1 that was considered as key factor to sustain the tumor growth for many cancers.

In the current study, we found increased alpha-2-HS-glycoprotein (FetuA) expression (1.6-fold) in tumor tissue whereas decreased concentration in blood sera of RCC (P= 0.0002) compared to healthy controls. Differential expression of alpha-2-HS-glycoprotein was reported in different cancers such as breast (Yi *et al*., 2009), lung (Niu *et al*., 2019), liver (Heo *et al*., 2018) and head and neck cancer (Thompson *et al*., 2014). Studies indicated down regulation of FetuA in sera of patients suffering from Familial Adenomatous Polyposis (Quaresima *et al*., 2008). Scientists reported that decreasing concentration of FETUA was directly linked to increased chronological age that is a prominent indicator of accelerated biological

aging (Teschendorff *et al*., 2010). In colorectal cancer up regulated serum FETUA was reported to inhibit the tumor progression by halting the binding of transforming growth factor-β1 to surface receptors thus inhibiting the TGF βsignal transduction which lead to the suppression of TGF β (Swallow *et al*., 2004) induced epithelial mesenchymal transition (Swallow *et al*., 2004; Li *et al*., 2014). Spatial information regarding to protein markers is interpreted by IHC by staining the tissues with dyes in predictive way. We selected A2M and FetuA proteins for validation in tissue samples by IHC to evaluate their significance for different treatment options. IHC discriminates the physiologies of tissues that are linked with weak prognosis and response towards treatment (Ring *et al*., 2009). IHC results depicted the positive staining of selected proteins for tumor tissues indicating the up regulated expression in tumor tissues compared to normal epithelium cells. Robust non-invasive cancer biomarkers can be developed by proteomic characterization of alternative body fluids in further details. Association of differential A2M and FetuA profiles with RCC observed in the present study may provide a better understanding of the molecular pathogenesis of the disease. Furthermore, linking such biomarkers with molecular therapies can improve treatment outcomes in future.

CONCLUSIONS AND RECOMMENDATIONS

The differential protein profile of FetuA and A2M associated with renal cell carcinoma provide a better way to understand the molecular mechanisms involved in tumor growth and progression. Tissue or fluid-based characterization of such biomarkers is the major target of proteomic technologies to establish the better diagnostics and treatment approaches. Furthermore, different protein markers linked to various molecular therapies help in understanding the major pathways involved in tumor progression.

ACKNOWLEDGEMENT

Authors are particularly thankful to the surgeons of the Public Hospitals of Lahore, Pakistan for providing tissue samples of RCC patients. Authors acknowledge the valuable assistance of Prof. Dr. Paul Stemmer from Wayne State University, USA, for his contribution to the MS analysis. Special recognition is extended to the Hillman Cancer Centre at the University of Pittsburgh for providing research facilities and invaluable environment.

Funding

The current study was funded by School of Biological Sciences and Higher Education Commission (HEC), Pakistan.

IRB approval

The study was approved by Institutional Ethical Review Board [ref No. 873/12].

Ethical statement

Tissue samples of male and female patients diagnosed with renal cell carcinoma (RCC) were collected from the local hospitals of Lahore, Pakistan during 2014–2018 with the consent according to the approved ethical guidelines.

Statement of conflict of interest

The authors have declared no conflict of interest.

REFERENCES

Al-Wajeeh, A.S., Salhimi, S.M., Al-Mansoub, M.A., Khalid, I.A., Harvey, T.M., Latiff, A. and Ismail, M.N., 2020. Comparative proteomic analysis of different stages of breast cancer tissues using ultra high performance liquid chromatography tandem mass spectrometer. *PLoS One*, **16**: 15. https://doi.org/10.1371/journal.pone.0227404

Baran, K. and Brzeziańska-Lasota, E., 2021. Proteomic biomarkers of non-small cell lung cancer patients. *Adv. Respir. Med*., **89**: 419-426. https://doi.org/10.5603/ARM.a2021.0089

Bradford, M.M., 1976. A rapid and sensitive method for the quantitation of microgram quantities of protein utilizing the principle of protein-dye binding. *Anal. Biochem*.,**72**: 248-254. https://doi.org/10.1016/0003-2697(76)90527-3

Clark, D.J., Dhanasekaran, S.M., Petralia, F., Pan, J., Song, X., Hu, Y., da Veiga Leprevost, F., Reva, B., Lih, T.-S.M. and Chang, H.Y., 2019. Integrated proteogenomic characterization of clear cell renal cell carcinoma. *Cell*, **179**: 964-983.

Clark, D.J. and Zhang, H., 2020. Proteomic approaches for characterizing renal cell carcinoma. *Clin. Proteom*., **17**: 28. https://doi.org/10.1186/s12014-020-09291-w

Drápela, S., Kvokačková, B., Fedr, R., Kurfürstová, D., Morong, M., Študent, V., van Weerden, W.M., Puhr, M., Culig, Z. and Bouchal, J., 2022. Pre-existing cell subpopulations in primary prostate cancers display surface fingerprint of docetaxel-resistant cells. *Am. J. Pathol*., **192**: 1321-1335. https://doi.org/10.1101/2021.01.28.428577

Dutta, I., Dieters-Castator, D., Papatzimas, J.W., Medina, A., Schueler, J., Derksen, D.J., Lajoie, G., Postovit,

L.-M. and Siegers, G.M., 2021. Adam protease inhibition overcomes resistance of breast cancer stem-like cells to γδ t cell immunotherapy. *Cancer Lett*., **496**: 156-168. https://doi.org/10.1016/j.canlet.2020.10.013

El-Shorbagy, S.H. and Alshenawy, H.A., 2017. Diagnostic utility of vimentin, cd117, cytokeratin-7 and caveolin-1 in differentiation between clear cell renal cell carcinoma, chromophobe renal cell carcinoma and oncocytoma. *J. Microsc. Ultrastruct*., **5**: 90-96. https://doi.org/10.1016/j.jmau.2016.07.005

Garcia-Fernandez, N., Jacobs-Cachá, C., Mora-Gutiérrez, J.M., Vergara, A., Orbe, J. and Soler, M.J., 2020. Matrix metalloproteinases in diabetic kidney disease. *J. clin. Med*., **9**: 472. https://doi.org/10.3390/jcm9020472

Gasparri, R., Sedda, G., Noberini, R., Bonaldi, T. and Spaggiari, L., 2020. Clinical application of mass spectrometry-based proteomics in lung cancer early diagnosis. *Proteomics Clin. appl*., **14**: e1900138. 1900138. https://doi.org/10.1002/prca.201900138

Heo, J.I., Yoon, D.W., Yu, J.H., Kim, N.H., Yoo, H.J., Seo, J.A., Kim, S.G., Choi, K.M., Baik, S.H. and Choi, D.S., 2018. Melatonin improves insulin resistance and hepatic steatosis through attenuation of alpha-2-hs-glycoprotein. *J. Pineal Res*., **65**: e12493. https://doi.org/10.1111/jpi.12493

Huang, H.L., Yao, H.S., Wang, Y., Wang, W.J., Hu, Z.Q. and Jin, K.Z., 2014. Proteomic identification of tumor biomarkers associated with primary gallbladder cancer. *World J. Gastroenterol*., **20**: 5511-5518. https://doi.org/10.3748/wjg.v20.i18.5511

Hussain, A., Dulay, P., Rivera, M.N., Aramouni, C. and Saxena, V., 2019. Neoplastic pathogenesis associated with cigarette carcinogens. *Cureus*,11: e3955. https://doi.org/10.7759/cureus.3955

Kwon, O.K., Ha, Y.S., Na, A.Y., Chun, S.Y., Kwon, T.G., Lee, J.N. and Lee, S., 2020. Identification of novel prognosis and prediction markers in advanced prostate cancer tissues based on quantitative proteomics. *Cancer Genom. Proteomic*., **17**: 195-208. https://doi.org/10.21873/cgp.20180

Lauer, D., Müller, R., Cott, C., Otto, A., Naumann, M. and Birkenmeier, G., 2001. Modulation of growth factor binding properties of a2-macroglobulin by enzyme therapy. *Cancer Chemother. Pharmacol*., **47**: 4-9. https://doi.org/10.1007/s002800170002

Li, C.J., Zhang, X. and Fan, G.W., 2014. Updates in colorectal cancer stem cell research. *J. Cancer Res. Ther*., **10**: 233-239. https://doi.org/10.4103/0973-1482.151449

Loomans-Kropp, H. and Umar, A., 2019. Increasing incidence of colorectal cancer in young adults. *J. Cancer Epidemiol*., **11**: 1-7. https://doi.org/10.1155/2019/9841295

Macklin, A., Khan, S. and Kislinger, T., 2020. Recent advances in mass spectrometry based clinical proteomics: Applications to cancer research. *Clin. Proteomics*., **17**: 1-25. https://doi.org/10.1186/s12014-020-09283-w

Mardamshina, M. and Geiger, T., 2017. Next-generation proteomics and its application to clinical breast cancer research. *Am. J. Pathol*., **187**: 2175-2184. https://doi.org/10.1016/j.ajpath.2017.07.003

McGinley, E., Lowe, G., Boulton-Jones, M., Forbes, C. and Prentice, C., 1983. Blood viscosity and haemostasis in the nephrotic syndrome. *Thromb. Haemost*., **49**: 155-157. https://doi.org/10.1055/s-0038-1657351

Mekkawy, A.H., Pourgholami, M.H. and Morris, D.L., 2014. Involvement of urokinase-type plasminogen activator system in cancer. *Med. Res. Rev.,* **34**: 918-956. https://doi.org/10.1002/med.21308

Mi, H., Muruganujan, A., Casagrande, J.T. and Thomas, P.D., 2013. Large-scale gene function analysis with the panther classification system. *Nat. Protoc*., **8**: 1551–1566.

Niu, L., Song, X., Wang, N., Xue, L., Song, X. and Xie, L., 2019. Tumor-derived exosomal proteins as diagnostic biomarkers in non-small cell lung cancer. *Cancer Sci*., **110**: 433-442. https://doi.org/10.1111/cas.13862

Quaresima, B., Crugliano, T., Gaspari, M., Faniello, M.C., Cosimo, P., Valanzano, R., Genuardi, M., Cannataro, M., Veltri, P. and Baudi, F., 2008. A proteomics approach to identify changes in protein profiles in serum of familial adenomatous polyposis patients. *Cancer Lett*., **272**: 40-52. https://doi.org/10.1016/j.canlet.2008.06.021

Ring, B.Z., Seitz, R.S., Beck, R.A., Shasteen, W.J., Soltermann, A., Arbogast, S., Robert, F., Schreeder, M.T. and Ross, D.T., 2009. A novel five-antibody immunohistochemical test for subclassification of lung carcinoma. *J. Mod. Hum. Pathol*., **22**: 1032-1043.

Rini, B.I., Motzer, R.J., Powles, T., McDermott, D.F., Escudier, B., Donskov, F., Hawkins, R., Bracarda, S., Bedke, J. and De Giorgi, U., 2021. Atezolizumab plus bevacizumab versus sunitinib for patients with untreated metastatic renal cell carcinoma and sarcomatoid features: A prespecified subgroup analysis of the immotion 151. *Clin. Trial.*

Eur. Urol., **79**: 659-662. https://doi.org/10.1016/j.eururo.2020.06.021

Shaw, R., Lokshin, A.E., Miller, M.C., Messerlian-Lambert, G. and Moore, R.G., 2022. Stacking machine learning algorithms for biomarker-based preoperative diagnosis of a pelvic mass. *Cancers* (Basel)., **14**: 1291. https://doi.org/10.3390/cancers14051291

Siegel, R.L., Miller, K.D., Fuchs, H.E. and Jemal, A., 2021. Cancer statistics, 2021. *CA Cancer J. Clin.*, **71**: 7-33. https://doi.org/10.3322/caac.21654

Stevenson, F., Sahota, S., Zhu, D., Ottensmeier, C., Chapman, C., Oscier, D. and Hamblin, T., 1998. Insight into the origin and clonal history of b-cell tumors as revealed by analysis of immunoglobulin variable region genes. *Immunol. Rev.*, **162**: 247-259. https://doi.org/10.1111/j.1600-065X.1998.tb01446.x

Surman, M., Kędracka-Krok, S., Hoja-Łukowicz, D., Jankowska, U., Drożdż, A., Stępień, E.Ł. and Przybyło, M., 2020. Mass spectrometry-based proteomic characterization of cutaneous melanoma ectosomes reveals the presence of cancer-related molecules. *Int. J. mol. Sci.*, **21**: 2934. https://doi.org/10.3390/ijms21082934

Swallow, C.J., Partridge, E.A., Macmillan, J.C., Tajirian, T., DiGuglielmo, G.M., Hay, K., Szweras, M., Jahnen-Dechent, W., Wrana, J.L. and Redston, M., 2004. A2hs-glycoprotein, an antagonist of transforming growth factor β *in vivo*, inhibits intestinal tumor progression. *Exp. mol. Med.*, **43**: 427-435.

Szklarczyk, D. and Jensen, L.J., 2015. Protein-protein interaction databases. Protein-protein interactions. *Methods mol. Biol.*, **1278**: 39-56. https://doi.org/10.1007/978-1-4939-2425-7_3

Teschendorff, A.E., Menon, U., Gentry-Maharaj, A., Ramus, S.J., Weisenberger, D.J., Shen, H., Campan, M., Noushmehr, H., Bell, C.G. and Maxwell, A.P., 2010. Age-dependent DNA methylation of genes that are suppressed in stem cells is a hallmark of cancer. *Genome Res.*, **20**: 440-446. https://doi.org/10.1101/gr.103606.109

Thieme, R., Kurz, S., Kolb, M., Debebe, T., Holtze, S., Morhart, M., Huse, K., Szafranski, K., Platzer, M. and Hildebrandt, T.B., 2015. Analysis of alpha-2 macroglobulin from the long-lived and cancer-resistant naked mole-rat and human plasma. *PLoS One*, **10**: e0130470. https://doi.org/10.1371/journal.pone.0130470

Thompson, P.D., Sakwe, A., Koumangoye, R., Yarbrough, W.G., Ochieng, J. and Marshall, D.R., 2014. Alpha-2 heremans schmid glycoprotein (ahsg) modulates signaling pathways in head and neck squamous cell carcinoma cell line sq20b. *Exp. Cell Res.*, **321**: 123-132. https://doi.org/10.1016/j.yexcr.2013.12.003

Yi, J.K., Chang, J.W., Han, W., Lee, J.W., Ko, E., Kim, D.H., Bae, J.Y., Yu, J., Lee, C. and Yu, M.H., 2009. Autoantibody to tumor antigen, alpha 2-hs glycoprotein: A novel biomarker of breast cancer screening and diagnosis. *Cancer Epidemiol. Biomarkers Prev.*, 18: 1357-1364. https://doi.org/10.1158/1055-9965.EPI-08-0696

Yoshino, S., Fujimoto, K., Takada, T., Kawamura, S., Ogawa, J., Kamata, Y., Kodera, Y. and Shichiri, M., 2019. Molecular form and concentration of serum α2-macroglobulin in diabetes. *Sci. Rep.*, **9**: 12927. https://doi.org/10.1038/s41598-019-49144-7